Growth on the reconstructed diamond (100) surface

ARTICLE *in* THE JOURNAL OF PHYSICAL CHEMISTRY · JANUARY 1993

Impact Factor: 2.78 · DOI: 10.1021/j100103a007

2 AUTHORS, INCLUDING:

Stephen Joel Harris
University of California, Berkeley
110 PUBLICATIONS **4,211** CITATIONS

Unclassif
SECURITY CLASSI

AD-A256 954

ION PAGE

Form Approved
OMB No. 0704-0188

1a. REPORT SECI Unclassified	1b. RESTRICTIVE MARKINGS
2a. SECURITY CLASSIFICATION AUTHORITY	3. DISTRIBUTION/AVAILABILITY OF REPORT Approved for public release
2b. DECLASSIFICATION/DOWN[illegible]ING SCHEDULE	
4. PERFORMING ORGANIZATION [illegible]PORT NUMBER(S) 5	5. MONITORING ORGANIZATION REPORT NUMBER(S) N00014-90-J-1386
6a. NAME OF PERFORMING ORGANIZATION Calif. Institute of Technology	6b. OFFICE SYMBOL (If applicable)
6c. ADDRESS (City, State, and ZIP Code) Mail Code 104-44 Pasadena, CA 91125	7a. NAME OF MONITORING ORGANIZATION Office of Naval Research (Dr. Dan Harris)
	7b. ADDRESS (City, State, and ZIP Code) Code 3854 Navel Air Warfare Center China Lake, CA 93555
8a. NAME OF FUNDING/SPONSORING ORGANIZATION Office of Naval Research	8b. OFFICE SYMBOL (If applicable)
8c. ADDRESS (City, State, and ZIP Code) 800 N. Quincy Street Arlington, VA 22217-5000	9. PROCUREMENT INSTRUMENT IDENTIFICATION NUMBER
	10. SOURCE OF FUNDING NUMBERS PROGRAM ELEMENT NO. / PROJECT NO. / TASK NO / WORK UNIT ACCESSION NO

DTIC
S A D
OCT 15 1992

(12)

11. TITLE (Include Security Classification)
Growth on the Reconstructed Diamond (100) Surface

12. PERSONAL AUTHOR(S)
S. J. Harris and D. G. Goodwin

13a. TYPE OF REPORT	13b. TIME COVERED	14. DATE OF REPORT (Year, Month, Day)	15. PAGE COUNT
technical	FROM _____ TO _____	92/10/01	33

16. SUPPLEMENTARY NOTATION

17. COSATI CODES			18. SUBJECT TERMS (Continue on reverse if necessary and identify by block number)
FIELD	GROUP	SUB-GROUP	

[illegible] approved
[illegible] sale; its
[illegible] unlimited.

19. ABSTRACT (Continue on reverse if necessary and identify by block number)

A thermochemical kinetics analysis has been carried out for growth on the (100)-(2x1):H diamond surface using a pair of previously proposed mechanisms which operate sequentially. Half of the growth on such a surface is accounted for by insertion into dimer bonds, while the other half is accounted for by addition across troughs between dimer bonds. The latter mechanism is slower and therefore controls the over-all growth rate on this surface. This result can explain the success that the latter mechanism has had in predicting growth rates in a variety of systems. We suggest that growth at step sites is favored on steric and thermochemical grounds and can account for atomically smooth surfaces on diamond.

92 1

398

20. DISTRIBUTION/AVAILABILITY OF ABSTRACT	21. ABSTRACT SECURITY CLASSIFICATION
☒ UNCLASSIFIED/UNLIMITED ☐ SAME AS RPT. ☐ DTIC USERS	Unclassified
22a. NAME OF RESPONSIBLE INDIVIDUAL David G. Goodwin	22b. TELEPHONE (Include Area Code) 818-356-4249 / 22c. OFFICE SYMBOL

DD Form 1473, JUN 86 — Previous editions are obsolete. — SECURITY CLASSIFICATION OF THIS PAGE
Unclassified

OFFICE OF NAVAL RESEARCH

Contract N00014-90-J-1386

R & T Project: irmt026

TECHNICAL REPORT NO.5

Growth on the Reconstructed Diamond (100) Surface

by

S. J. Harris and D. G. Goodwin

Prepared for Publication

in

Journal of Physical Chemistry

Division of Engineering and Applied Science
California Institute of Technology
Pasadena, California 91125

October 1, 1992

Growth on the Reconstructed Diamond (100) Surface

by

Stephen J. Harris

Physical Chemistry Dept., General Motors Research Labs

30500 Mound Road, Box 9055, Warren, MI 48090-9055

and

D. G. Goodwin

Division of Engineering and Applied Science

California Institute of Technology

Pasadena, CA 91125

Abstract

A thermochemical kinetics analysis has been carried out for growth on the (100)-(2×1):H diamond surface using a pair of previously proposed mechanisms which operate sequentially. Half of the growth on such a surface is accounted for by insertion into dimer bonds, while the other half is accounted for by addition across troughs between dimer bonds. The latter mechanism is slower and therefore controls the overall growth rate on this surface. This result can explain the success that the latter mechanism has had in predicting growth rates in a variety of systems. We suggest that growth at step sites is favored on steric and thermochemical grounds and can account for atomically smooth surfaces on diamond.

Introduction

In the past few years several detailed growth mechanisms have been proposed to explain the chemical vapor deposition (CVD) of diamond films [1–10]. In general, these models have used the formal resemblance between the bonding and structure in diamond and in alkanes to postulate [6] that chemistry on the diamond surface could be understood in terms of the very well known chemistry of alkanes. In effect, the assumption is made that the chemistry of a diamond surface is controlled by the local electronic environment, as is true for alkanes, and that bulk band structure and surface states play no role. If this postulate is valid, then considering all that is known about alkane chemistry, we may be able to understand CVD diamond growth at a level of detail beyond that for any other CVD process.

Considerable research in the field has been aimed at determining the "growth" species, i.e., the gas phase species directly responsible for diamond formation [11, 12], and recent experiments have demonstrated that the CH_3 radical is the primary growth species in the CVD systems that have been examined [13–19]. One proposed chemical kinetics mechanism [2], which takes CH_3 as the growth species, successfully predicts [20–22], experimental growth rates for both RF [21] and DC [23] plasma torches, for flames at low and atmospheric pressure [15, 24, 25], and for filament systems as a function of pressure and composition [16, 17], without the use of adjustable parameters. Its predictions are compared to experiment in Figure 1. The ability of the model to predict the relative growth rates for these very different systems is striking. However, we have pointed out [2] that the near-perfect *absolute* agreement is fortuitous—our estimated uncertainty is a couple of orders of magnitude in either direction [2]. This is because there is uncertainty not only in gas phase rate and thermodynamic parameters themselves, but also in how these parameters should be converted for use with surface kinetics. As discussed previously [2], the mechanism

models the diamond surface with the 9-carbon molecule bicyclononane (BCN), which in effect takes the diamond surface to be an unreconstructed (100) surface. However, it is unlikely that such a surface would be stable because of very large $H - H$ steric repulsions [26]. Recent STM and AFM experiments have shown [27–29] that diamond surfaces can be rather rough on an atomic scale, but at least some of the surface reconstructs to the (100)-(2×1):H form [28, 30, 31]. On this surface each carbon atom is bonded twice to carbons in the bulk, once to a surface hydrogen, and once to a neighboring surface carbon making a "dimer" and forming a 5-membered ring, as seen in Figure 2. A quantitative analysis of the steric forces on various (100) surfaces shows that this dimer reconstruction substantially reduces surface stress compared to the unreconstructed surface [26, 32]. In this paper we propose that the growth kinetics on the (100)-(2×1):H surface can be understood by combining two different mechanisms—a "trough" mechanism (identical to the BCN mechanism) and a "dimer" mechanism—which operate sequentially on the two types of sites present on this surface. This picture of growth can explain the success that the BCN mechanism has enjoyed.

Analysis

Any acceptable diamond growth mechanism must be both fast enough to explain observed growth rates and thermodynamically favorable enough so that the overall reaction in the reverse direction (etching) is negligible [2, 33, 34]. The latter requirement comes from the experimental observation that etching by atomic hydrogen is extremely slow. In this section we describe our analysis for the thermochemistry and kinetics of proposed growth mechanisms which satisfy these conditions.

Structure of the Model Compound

The first step is to choose a model structure to represent the diamond crystal and surface. Use of very large model structures is a requirement if steric energies—which can be quite large—are to be calculated accurately. This is because the calculation must take into account the fact that lattice atoms close to a surface reaction site may move somewhat to relieve steric repulsions, but it must also take into account that the crystal as a whole is extremely rigid. For estimating steric energies, we used the crystal slab shown in Figure 2, which is 1.6 by 1.6 by 0.6 nm (8 layers) thick and contains 330 carbon atoms and 20 surface dimer bonds. Reaction takes place near the center of the slab. Although this crystal is relatively large, when finding the steric energy it was necessary to hold twenty atoms at the base and edges of the crystal fixed in order to prevent the crystal from flexing due to the large surface tensile stress induced by the dimers. For estimating heat capacities and entropies we used a smaller (160 carbon atoms) 1.0 by 0.6 by 0.6 nm thick diamond slab because of limitations of the computer program.

Gas Phase Species Concentrations

For the models discussed here we assume that growth occurs from reaction of the CH_3 radical at the diamond surface. We take gas phase concentrations from measurements and modeling [12, 35–37]. For our typical filament-assisted growth conditions with the substrate temperature 1200 K and the pressure 20 torr we have $X_H = 2 \times 10^{-3}$ and $X_{CH_3} = 2 \times 10^{-4}$, where X_i is the mole fraction of species i.

Rate Constants

Rate constants for the gas-surface reactions that appear in these mechanisms have not been measured. In order to estimate their values we have made the assumption [4] that the reaction cross section per surface site is equal to the reaction cross section per equivalent site in a prototype gas phase reaction. According to our analysis for

an abstraction by a gas phase species of mass m_g this assumption leads to [4]

$$k_s = k_g n_s [\mu/m_g]^{1/2},$$

where k_s and k_g are the surface and gas phase rate constants, respectively, μ is the reduced mass of the reactants in the prototype gas phase reaction, and the symmetry number n_s is the number of identical sites on the surface structure being examined. In other words, the surface rate constant equals the gas phase rate constant corrected for the effect of collision frequency and for symmetry. We use the same approach for radical recombination reactions, with one difference. We consider the radical site on the gas phase molecule to be equivalent to two surface radical sites because the nearly-planar gas phase radical has two equally probable sides for reaction, whereas the surface radical has only 1 side from which reaction can occur. Thus, for radical recombination we have

$$k_s = 0.5\, n_s k_g [\mu/m_g]^{1/2}.$$

Assuming a constant reaction cross section neglects some factors which may affect the surface rate constant. Steric hindrances and reaction barriers might differ on the surface from those of the prototype gas phase reactions. Also, transition state theory shows that the pre-exponential factor is determined by the entropy change $\Delta S^{\ddagger}$ in forming the activated complex; even if the reaction potential surface is the same for the prototype and surface reactions, differences in the translational and rotational contributions to $\Delta S^{\ddagger}$ may alter the pre-exponential factor somewhat. These effects are ignored here, since they are difficult to estimate accurately and are not expected to qualitatively affect our conclusions.

The rate constants are shown in Tables 1 and 2. (Definitions of the species are given below.) Two surface isomerization reactions in Table 1, G and H, are treated differently. We do not expect a significant barrier for Reactions G, so we have assigned it a large rate constant which simply insures that this reaction is in partial equilibrium.

The rate constant for Reaction H has been estimated by Musgrave, Goddard, and Harris [38] using *ab initio* quantum techniques.

Thermochemistry

We estimate values for the enthalpy change ΔH and entropy change ΔS in order to determine $\Delta G = \Delta H - T\Delta S$ for each reaction. From ΔG we can calculate rate constants for reverse reactions, which are related to the forward rate constants by

$$K_{eq} = k_f/k_r = e^{-\Delta G/RT},$$

where K_{eq} is the equilibrium constant. (Thermochemical quantities are tabulated for standard states of 1 atmosphere, whereas we are using concentration units. For reactions in which the number of moles changes, k_r must be multiplied by a factor which converts between atmospheres and moles/cm^3.)

To estimate thermodynamic parameters we have suggested the use of molecular mechanics [34]. With this technique, a force field is established that describes the interaction of every atom in the system with every other atom. In general, both the functional forms for the interactions and the associated coefficients are chosen empirically. A number of force fields have been proposed for carbon atoms [39–41], but the most widely used and extensively tested force fields for obtaining thermodynamic quantities are MM2 [42] and MM3 [43], which we use in this paper. These force fields, which were designed specifically to estimate steric repulsions in highly strained alkanes, give each bond a set of force constants (e.g., stretching, bending, torsion) for displacement from "natural" lengths and angles, and give each atom van der Waals attractions and repulsions to the other atoms in the system. Our codes use the MM2 or MM3 force fields to adjust the position of every atom in the system in order to minimize the total strain energy E_{strain}, which is the result of bonds bending, stretching, and twisting in response to van der Waals attractions and repulsions. The heat of formation H_f for a molecule is obtained by combining this calculated E_{strain}

with bond enthalpies H_{bond} calculated from an associated group additivity scheme. MM2 and MM3 predict H_f of even very crowded and highly strained molecules to within typically 0.5 kcal/mole (0.02 eV/molecule), which is not much greater than the experimental error [42, 43]. On the other hand, since MM3 is a purely empirical force field and has not been calibrated against a diamond surface, we do not expect the predicted energetics to be so accurate for the present work. For example, we estimate that fixing atoms at the base and edges of the model compound (see above) introduces an uncertainty of around 1 or 2 kcal/mole in relative heats of formation. (Only relative—not absolute—heats of formation appear in the analysis.) The MM3 force field can also calculate vibrational frequencies. For stable structures we use the enthalpy calculations from MM3. Since the radical force field in that code has not yet been finalized [44], we use the MM2 force field to estimate the difference in the heats of formation of stable species and radical species with a hydrogen removed. Heats of formation calculated by MM2 and MM3 differ significantly only where there are non-bonded H-H distances less than 0.2 nm [43], which occur for the species C_5M and C_6HM. For these cases, an error of 1 to 2 kcal/mole may be introduced by our use of MM2. The entropy is calculated primarily by using the MM3 code. However, we have also included a symmetry term $-R\ln n_s$ to take into account the presence of identical atoms for some of the surface structures, and we treat $-CH_3$ and $-CH_2^*$ groups as free rotors. Treating these as free rotors is a good approximation, since the barriers to rotation are found to be typically less than 1 kcal/mole. Thermodynamic quantities calculated at 1200 K for the two mechanisms considered, relative to the C_5 starting structure (see below), are shown in Table 3 and 4.

Reaction Mechanisms

Carbon atoms can add onto the (100)-(2×1):H surface at two types of sites, inserting into dimer bonds or adding across troughs between dimer bonds. To complete

a new monolayer, half of the carbons must add to the dimer sites and half to the trough sites. The added carbons may then dimerize with their neighbors, forming a new (2x1) surface on a new layer, with dimer rows orthogonal to the original rows. Recently, Garrison and co-workers [45] have proposed a mechanism for insertion into dimer bonds which involves exclusively reactions that have low activation barriers and well-known analogs in hydrocarbon chemistry. (Another proposed mechanism for insertion into dimer bonds [46] includes a step with a 3-center transition state. Since the barrier at that transition state is calculated [46] to be very high, it is not considered further.) For addition across the troughs we use the bicyclononane (BCN) mechanism, which was originally proposed [2] to explain growth on the unreconstructed (100) surface. Although the atoms making up a trough are isomorphic to those on an unreconstructed (100) surface, on the (100)-(2×1):H surface the strain energy associated with this structure is substantially reduced. Thus, the BCN mechanism can be applied more realistically to troughs on the (100)-(2×1):H surface.

Dimer mechanism

The steps in the dimer mechanism of Garrison et al. [45] are reviewed in Table 1. This mechanism begins with the dimer structure on the (100)-(2×1):H surface, which we denote C_5 (Figure 3a) because of the presence of 5-membered rings. In the initial step (Reaction A) a surface hydrogen is abstracted by a gas phase H atom forming the tertiary surface radical C_5^* and the H_2^{gas} molecule. Either H^{gas} (Reaction B) or CH_3^{gas} (Reaction C) can recombine at this radical site to give C_5 or C_5M, respectively. A hydrogen atom from the methyl group of C_5M can be abstracted to give C_5M^* (Reaction D), which in turn may react with H^{gas} (Reactions E or F). In the next step (Reaction G) C_5M^* isomerizes to C_d^* (Figure 3b), a species which contains both a radical site and a double bond. Reaction G is called a β scission reaction [47] because the C-C bond two carbons away (or "β") from the radical site is broken during this isomerization reaction. (Two other C-C bonds can also break via a β

scission reaction; products of those reactions are not considered here.) The radical carbon in C_d^* can react with either end of the carbon-carbon double bond. Addition to the end closest to the bulk diamond reverses Reaction G, while addition to the other end forms the C_6^* species (Reaction H, Figure 3c). Finally, C_6^* and C_6 interconvert by Reactions I and J. We note that a total of two hydrogen abstraction reactions are necessary to form C_6 from C_5.

Trough Mechanism

The steps involved in adding carbon across the trough on the (100)-(2×1):H surface are identical to those proposed previously in the trough mechanism [2, 3] (except that formation of long-chain hydrocarbons, Reaction j, is not considered here), and they are shown in Table 2. Briefly, a methyl radical adds at a radical site formed from abstraction of one or both of the trough hydrogens (see Figure 3e). This step is followed either by abstraction of the other trough hydrogen and one of the methyl hydrogens (Reactions d or f and k after Reaction c) or by abstraction of a methyl hydrogen (Reaction l after Reaction s) to give the C_6B structure, which has a carbon atom that bridges the trough. For reasons discussed below, we allow the trough mechanism to occur only adjacent to C_6-type sites just formed by the dimer mechanism, as shown in Figure 3e. Thus, the starting structure is called C_6HH, which refers to the two H atoms pointing toward each other across the trough and next to a newly-formed C_6 species. The final bridged structure is called C_6B. We note that a total of three hydrogen abstraction reactions are necessary.

Results

Dimer mechanism

The time dependence for the dimer mechanism is calculated by integrating the rate equations for Reactions A through J. Initially, the fraction of the dimer sites which are C_5 is 1.0, and the fraction of all other species in the mechanism is 0. The

calculation shows the surface rapidly reaches steady state, within less than 100 ms. However, there are no irreversible steps in this mechanism, since those steps which have a large enthalpy reduction also have a substantial reduction in entropy. The result is that the reaction sequence is reversible, in conflict with experiment.

This situation can be easily remedied by adding Reactions K, L, and M to the mechanism, which creates a dimer on a new layer, which we call Layer $n+1$. The resulting structure, C_6HH, is shown in Figure 3e. C_6HH is generated when a C_6 species is formed directly in front of or behind (eclipsing) a C_6T^* species, which has a radical site at the top carbon (Figure 3d),

$$C_6 + C_6T^* + H^{gas} = C_6HH + H_2^{gas}. \qquad \text{(M)}$$

Because $\Delta G \ll 0$ for Reaction M, it is effectively irreversible (assuming that we have not omitted some other etching reactions of C_6HH which could convert it back to C_5), and C_6HH ultimately covers half a monolayer. The rate of formation of that half-monolayer would correspond to an effective linear growth rate of around 7 microns/hour. However, since after approximately 100 ms growth is effectively stopped until the trough sites can be filled in, the actual growth rate is limited by whichever process is slower.

Trough Mechanism

Although the dimer mechanism including Reactions K through M is relatively fast and irreversible, it accounts for growth only on dimer sites; the trough mechanism adds carbon atoms at the sites which separate the dimers. We take as the starting point for the trough mechanism the structure C_6HH produced by the dimer mechanism, that is, one dimer already formed on Layer $n+1$. Because of the large negative values of ΔG for Reactions k and l, formation of C_6B is irreversible via the trough mechanism. Furthermore, C_6B cannot react back to C_6HH via the reverse of the dimer mechanism since formation of a dimer-type bond across the trough is not

energetically feasible. C_6B formation is followed by a rapid reactions analogous to Reactions K through M of the dimer mechanism in which a pair of eclipsed C_6B species reacts to form a dimer bond on Layer $n+1$. Thus, the combined dimer/trough mechanism starts with two dimer bonds and creates a new surface containing two dimer bonds, one each from the dimer and trough parts of the mechanism.

There are a couple of approximations implicit in this picture that should be pointed out. First, in order to keep the reaction mechanism manageable we have made an independent sub-unit approximation, assuming that the kinetic and thermodynamic parameters for each dimer-trough pair are independent of the status at neighboring dimer-trough pairs. Second, we note that when all of the dimer-trough pairs have reacted the new surface is again a (100)-(2×1):H surface, but it has not been returned to a structure identical to the starting structure because the dimer bonds formed on Layer $n+1$ are at right angles to those on Layer n. In fact, because of the *abcabc*... structure of the diamond lattice, Layer n is not reproduced until Layer $n+4$. However, the structures of each of these layers are congruent—they are merely shifted or rotated. Thus, we assume that the growth rate of each layer between n and $n+4$ takes place at the same rate.

The most important difference between the two mechanisms from the point of view of kinetics is that the trough mechanism is considerably slower, due partly to the additional H atom abstraction that must occur with the trough mechanism. The steady state linear growth rate of the combined mechanism is calculated to be 0.5 μm/hr, limited by the trough portion of the mechanism. This rate is controlled by two factors. The first factor is the rate of addition of CH_3 to the surface, which is determined by the fraction of the surface sites which are radicals and by the rate constants for Reactions c and s. The second factor is the fraction of the CH_3 radicals which desorb before they can be incorporated into the crystal. For example, the reverse of Reaction c, in which the CH_3 group from C_6HM desorbs, is several times

faster than Reactions d or f, in which the surface growth processes continue. In contrast, the reverse of Reaction s, in which the CH_3 from C_6^*M desorbs, is an order of magnitude slower than the irreversible formation of C_6B in Reaction l. This difference is a consequence of the considerably greater steric repulsion in C_6HM compared to C_6^*M, which leads to spontaneous CH_3 desorption lifetimes at 1200 K of 100 μs and 11 ms for the two species, respectively. As a result, most of the C_6B which is formed passes through Reaction s rather than Reaction c, even though C_6^{**} is a relatively high energy species. The hydrogen atom concentration also plays a role, since irreversible incorporation of carbon into the lattice requires abstractions by gas phase H atoms which compete with methyl desorption. We have published previously our predictions for the effect of H atom concentration on growth rates [3, 4], but we are not aware of any experimental data which test them.

Discussion

Since a (100)-(2×1):H surface contains equal numbers of dimer and trough sites, the dimer and trough mechanisms ultimately contribute equally to growth. However, steric repulsion controls how and when these mechanisms play their roles. The interactions between these mechanisms can be discussed with reference to the drawing in Figure 4, which labels dimer sites as a, c, e, and g, and trough sites as b, d, f, and h.

Growth of Layer $n+1$ can commence only with the dimer mechanism and not the trough mechanism. This is because spanning a trough giving a hypothetical C_5B structure would create highly strained bonds and would be unstable because the C–C bonds would have to be too long. Thus, the first reactions are reversible formation of C_6 species on the dimer sites a, c, e, or g followed by the irreversible formation of C_6HH. C_6HH sites will not in general exist simultaneously at a and c or at e and g because that would lead to large H–H steric repulsions across the trough. This

would shift the reactions

$$C_5M^* \rightleftharpoons C_d^* \rightleftharpoons C_6^*$$

strongly to the left and slow the dimer mechanism. Therefore, once a new dimer bond C_6HH forms at c and g, for example, reaction at a and e to make another C_6HH structure there is unlikely. However, the presence of a C_6HH species at c and g shortens the distance across the trough, which allows troughs b, d, f, and h to be spanned. Thus, C_6B structures are formed with the trough mechanism, and these react with each other to form additional dimer bonds on Layer $n+1$. At this point, with the trough hydrogens eliminated, the dimer mechanism rapidly adds carbon at a and e. Thus, growth on the (100)-(2×1):H surface occurs in a coordinated fashion, first up and down rows of (eclipsed) dimers, then up and down adjacent rows of (eclipsed) troughs, then up and down the remaining rows of (eclipsed) dimers.

According to our analysis, the steady state growth rate at dimer sites is considerably faster than at trough sites. Since a complete new layer cannot form until addition has taken place at each trough site, the trough mechanism is rate limiting. This result may provide an explanation for the observation that experimental growth rates can be calculated with the trough mechanism, as seen in Figure 1.

Atomically Smooth Surfaces on Diamond

In this work we have represented the surface by an ensemble of independent sub-units consisting of a pair of dimer bonds next to a pair of troughs, such as sites a, b, e, and f (see Figure 3a). To some extent this representation is adequate. For example, the difference in steric energy between C_5 and C_5M changes by only around 1 kcal/mole, depending on whether or not a C_6HH structure is adjacent to the C_5. Furthermore, the independent sub-unit representation does allow us to predict a certain

amount of coordination between subunits. For example, because of the alternating nature of the dimer/trough mechanism, we found that neighboring dimer rows cannot grow until the trough between them has been spanned. However this approach does not account for the relatively smooth surfaces that have sometimes been observed over long ranges on the (100)-(2×1):H surface [28,30,31]. On metals and some other types of crystals, smooth surfaces are the result of loosely bound adatoms diffusing to steps and kinks, which lowers their energy (by increasing their coordination numbers) and leads preferentially to growth at those sites. This process produces fast lateral growth and smooth surfaces. In contrast, it is unlikely that chemically bound hydrocarbon adsorbates would be mobile on a hydrogenated diamond surface [48]. Furthermore, the coordination number of hydrocarbon adsorbates is unaffected by whether they are bound at step or terrace sites. Thus, diffusion of adsorbates to steps and kinks would not provide a mechanism for explaining atomically smooth growth on diamond.

We suggest instead that steric and thermochemical factors can favor growth at step sites over growth on smooth surfaces. For example, we have already shown that growth on atomically smooth (111) surfaces is highly unlikely with a straightforward abstraction-addition mechanism [34]. As we have pointed out above, smooth unreconstructed (100) surfaces may well not exist, but we found previously [3] that methyl radical addition at step sites with (100) character can readily occur because these sites are in general less sterically crowded. Similarly, addition to (110)- or dimer/trough-type sites may be sterically easier at steps than on flat surfaces. If growth intermediates are more stable at step and kink sites, growth would occur preferentially there for the same reason that growth with the trough mechanism occurs preferentially through C_6^*M rather than through C_6HM. The result would then be fast lateral growth leading to smooth surfaces.

Acknowledgments

Valuable discussions with Professor Mark D'Evelyn of Rice University are gratefully acknowledged. This work has been supported, in part, by the Office of Naval Research under contract N00014-90-J-1386.

REFERENCES

[1] J. C. Angus and C. C. Hayman, Science **241**, 913 (1988).

[2] S. J. Harris, Applied Physics Letters **56**, 2298 (1990).

[3] S. J. Harris and D. N. Belton, Thin Solid Films **212**, 193 (1992).

[4] D. N. Belton and S. J. Harris, Journal of Chemical Physics **96**, 2371 (1992).

[5] M. Frenklach and H. Wang, Physical Review B **43**, 1520 (1991).

[6] M. Frenklach and K. E. Spear, Journal of Materials Research **3**, 133 (1988).

[7] D. Huang, M. Frenklach, and M. Maroncelli, Journal of Physical Chemistry **92**, 6379 (1988).

[8] M. E. Coltrin and D. S. Dandy, Journal of Applied Physics (submitted).

[9] W. A. Yarbrough, in *Diamond Optics IV*, edited by A. Feldman and S. Holly (Proc. SPIE, 1991), p. 1534.

[10] P. Deak, J. Giber, and H. Oechsner, Surface Science **250**, 287 (1991).

[11] S. J. Harris, A. M. Weiner, and Thomas A. Perry, Applied Physics Letters **53**, 1605 (1988).

[12] D. G. Goodwin and G. G. Gavillet, Journal of Applied Physics **68**, 6393 (1990).

[13] C. J. Chu, M. P. D'Evelyn, R. H. Hauge, and J. L. Margrave, Journal of Applied Physics **70**, 1695 (1991).

[14] C. E. Johnson, W. A. Weimer, and F. M. Cerio, Journal of Materials Research **7**, 1427 (1992).

[15] Y. Matsui, H. Yabe, and Y. Hirose, Japanese Journal of Applied Physics **29**, 1552 (1990).

[16] S. J. Harris, A. M. Weiner, and T. A. Perry, Journal of Applied Physics **70**, 1385 (1991).

[17] S. J. Harris and A. M. Weiner, Thin Solid Films **212**, 201 (1992).

[18] L. Schafer, M. Sattler, and C.-P. Klages, "Upscaling of the hot-filament CVD process for deposition of diamond films on large-area substrates", Applied Diamond Conference, August, 1991, Auburn, Alabama, poster.

[19] W. A. Yarbrough, K. Tankala, and T. DebRoy, Journal of Materials Research **7**, 379 (1992).

[20] D. G. Goodwin, Applied Physics Letters **59**, 277 (1991).

[21] T. G. Owano, D. G. Goodwin, C. H. Kruger, and M. A. Cappelli, *Second International Conference on the New Diamond Science and Technology* (Washington, DC, 1990), p. 497. Paper 7.2.

[22] D. G. Goodwin, unpublished.

[23] K. R. Stalder and R. L. Sharpless, Journal of Applied Physics **68**, 6187 (1990).

[24] Y. Matsui, A. Yuuki, M. Sahara, and Y. Hirose, Japanese Journal of Applied Physics **28**, 1718 (1989).

[25] N. G. Glumac and D. G. Goodwin, Thin Solid Films **212**, 122 (1992).

[26] Y. L. Yang and M. P. D'Evelyn, Journal of the Americal Chemical Society **114**, 2796 (1992).

[27] M. P. Everson and M. A. Tamor, Journal of Vacuum Science and Technology A **9**, 1570 (1991).

[28] L. F. Sutcu, C. J. Chu, M. S. Thompson, R. H. Hauge, J. L. Margrave, and M. P. D'Evelyn, Journal of Applied Physics **71**, 5930 (1992).

[29] V. Baranauskas, M. Fukui, C. R. Rodrigues, and N. Parizotto, Applied Physics Letters **60**, 1567 (1992).

[30] T. Tsuno, T. Imai, Y. Nishibayashi, K. Hamada, and N. Fujimori, Japanese Journal of Applied Physics **30**, 1063 (1991).

[31] H. Sprang, H. G. Busmann, and I. V. Hertel, *Second European Conference on Diamond, Diamond-like and related coatings* (Nice, France, 1991), p. 443.

[32] Y. L. Yang and M. P. D'Evelyn, Journal of Vacuum Science and Technology A,

(1992).

[33] S. J. Harris and D. N. Belton, Japanese Journal of Applied Physics **30**, 2615 (1991).

[34] S. J. Harris, D. N. Belton, and R. J. Blint, Journal of Applied Physics **70**, 2654 (1991).

[35] W. L. Hsu, *Proceedings of the Electrochemistry Society* (Electrochemical Society, Pennington, NJ, Pennington, NJ, 1991).

[36] S. J. Harris and A. M. Weiner, Journal of Applied Physics **67**, 6520 (1990).

[37] F. G. Celii and J. E. Butler, Applied Physics Letters **54**, 1031 (1989).

[38] C. Musgrave, W. A. Goddard, and S. J. Harris, unpublished.

[39] E. Pearson, T. Takai, T. Halicioglu, and W. A. Tiller, Journal of Crystal Growth **70**, 33 (1984).

[40] J. Tersoff, Physical Review Letters **56**, 632 (1986).

[41] D. W. Brenner, Physical Review B **42**, 9458 (1990).

[42] N. L. Allinger, Journal of the Americal Chemical Society **99**, 8127 (1977).

[43] J.-H. Lii and N. L. Allinger, Journal of the Americal Chemical Society **111**, 8551 (1989).

[44] R. Lee, University of Georgia, Private communication.

[45] B. J. Garrison, E. J. Dawnkaski, D. Srivastava, and D. W. Brenner, Science **255**, 835 (1992).

[46] D. Huang and M. Frenklach, Journal of Physical Chemistry **96**, 1868 (1992).

[47] E. I. Axelsson, K. Brezinsky, F. L. Dryer, W. J. Pitz, and C. K. Westbrook, *Twenty-first Symposium (International) on Combustion* (The Combustion Institute, Seattle, WA, 1986), p. 783.

[48] S. P. Mehandru and Alfred B. Anderson, Journal of Materials Research **5**, 2286 (1990).

Table 1

DIMER MECHANISM

REACTION				ΔG^a_{1200}	k^b
A.	$C_5 + H^{gas}$	$\rightleftharpoons$	$C_5^* + H_2^{gas}$	−14.2	$2.52 \times 10^{14} e^{-7300/RT}$
B.	$C_5^* + H^{gas}$	$\rightleftharpoons$	C_5	−59.5	1.0×10^{13}
C.	$C_5^* + CH_3^{gas}$	$\rightleftharpoons$	C_5M	−30.2	5.0×10^{12}
D.	$C_5M + H^{gas}$	$\rightleftharpoons$	$C_5M^* + H_2^{gas}$	−16.9	$2.81 \times 10^7 T^2 e^{-7700/RT}$
E.	$C_5M^* + H^{gas}$	$\rightleftharpoons$	C_5M	−57.6	1.0×10^{13}
F.	$C_5M^* + H^{gas}$	$\rightleftharpoons$	$C_5^* + CH_3^{gas}$	−27.4	3.0×10^{13}
G.	C_5M^*	$\rightleftharpoons$	C_d^*	+4.3	1.0×10^{13}
H.	C_d^*	$\rightleftharpoons$	C_6^*	−21.2	$6.9 \times 10^{12} e^{-8100/RT}$
I.	$C_6^* + H^{gas}$	$\rightleftharpoons$	C_6	−48.5	1.0×10^{13}
J.	$C_6 + H^{gas}$	$\rightleftharpoons$	$C_6^* + H_2^{gas}$	−25.2	$1.26 \times 10^{14} e^{-7300/RT}$
K.[c]	$C_6 + H^{gas}$	$\rightleftharpoons$	$C_6T^* + H_2^{gas}$	−22.9	$9.0 \times 10^6 T^2 e^{-5000/RT}$
L.[c]	$C_6T^* + H^{gas}$	$\rightleftharpoons$	C_6	−50.8	1.0×10^{13}
M.[c]	$C_6T^* + C_6 + H^{gas}$	$\rightleftharpoons$	$C_6HH + H_2^{gas}$	−61.1	$1.8 \times 10^7 T^2 e^{-5000/RT}$

a. units are kcal/mole

b. units are cm^3, moles, seconds

c. Analogous reactions can be written for C_6^*.

Table 2

TROUGH MECHANISM

REACTION			ΔG^{1200}	k
$a.\ C_6HH + H^{gas}$	$\rightleftharpoons$	$C_6H^{\bullet} + H_2^{gas}$	-16.1	$1.3 \times 10^{14} e^{-7300/RT}$
$b.\ C_6H^{\bullet} + H^{gas}$	$\rightleftharpoons$	C_6HH	-57.6	1.0×10^{13}
$c.\ C_6H^{\bullet} + CH_3^{gas}$	$\rightleftharpoons$	C_6HM	-20.6	5.0×10^{12}
$d.\ C_6HM + H^{gas}$	$\rightleftharpoons$	$C_6^{\bullet}M + H_2^{gas}$	-30.3	$1.3 \times 10^{14} e^{-7300/RT}$
$e.\ C_6^{\bullet}M + H^{gas}$	$\rightleftharpoons$	C_6HM	-64.0	1.0×10^{13}
$f.\ C_6HM + H^{gas}$	$\rightleftharpoons$	$C_6HM^{\bullet} + H_2^{gas}$	-19.1	$2.8 \times 10^{7} T^2 e^{-7700/RT}$
$g.\ C_6HM^{\bullet} + H^{gas}$	$\rightleftharpoons$	C_6HM	-54.6	1.0×10^{13}
$h.\ C_6HM^{\bullet}$	$\rightleftharpoons$	$C_6^{\bullet}M$	-11.2	1.0×10^{8}
$i.\ C_6HM^{\bullet} + H^{gas}$	$\rightleftharpoons$	$C_6H^{\bullet} + CH_3^{gas}$	-34.0	3.0×10^{13}
$k.\ C_6HM^{\bullet} + H^{gas}$	$\rightleftharpoons$	$C_6B + H_2^{gas}$	-67.3	$1.3 \times 10^{14} e^{-7300/RT}$
$l.\ C_6^{\bullet}M + H^{gas}$	$\rightleftharpoons$	$C_6B + H_2^{gas}$	-56.1	$2.8 \times 10^{7} T^2 e^{-7700/RT}$
$m.\ C_6HH + H^{gas}$	$\rightleftharpoons$	$C_6^{\bullet}H + H_2^{gas}$	-22.3	$1.3 \times 10^{14} e^{-7300/RT}$
$n.\ C_6^{\bullet}H + H^{gas}$	$\rightleftharpoons$	C_6HH	-51.4	1.0×10^{13}
$o.\ C_6H^{\bullet} + H^{gas}$	$\rightleftharpoons$	$C_6^{\bullet\bullet} + H_2^{gas}$	-18.7	$1.3 \times 10^{14} e^{-7300/RT}$
$p.\ C_6^{\bullet\bullet} + H^{gas}$	$\rightleftharpoons$	$C_6H^{\bullet}$	-55.0	1.0×10^{13}
$q.\ C_6^{\bullet}H + H^{gas}$	$\rightleftharpoons$	$C_6^{\bullet\bullet} + H_2^{gas}$	-12.5	$4.5 \times 10^{6} T^2 e^{-5000/RT}$
$r.\ C_6^{\bullet\bullet} + H^{gas}$	$\rightleftharpoons$	$C_6^{\bullet}H$	-61.2	1.0×10^{13}
$s.\ C_6^{\bullet\bullet} + CH_3^{gas}$	$\rightleftharpoons$	$C_6^{\bullet}M$	-32.2	5.0×10^{12}
$t.\ C_6H^{\bullet}$	$\rightleftharpoons$	$C_6^{\bullet}H$	-6.2	1.0×10^{8}

Table 3

THERMOCHEMISTRY FOR DIMER MECHANISM

SPECIES	H^a kcal/mole	S^a cal/mole-Kelvin	$G^{a,b}$ kcal/mole	n_s
C_5	0.0	0.0	0.0	2
C_5^*	+44.0	−0.1	+44.1	1
C_5M	9.1	+20.5	−15.4	3
C_5M^*	+51.3	+20.4	+26.8	2
C_d^*	+56.2	+20.9	+31.1	1
C_6^*	+27.9	+15.0	+9.9	1
C_6	−5.8	+14.5	−23.2	2
C_6T^*	+32.8	+17.2	+12.2	1
H^{gas}	56.6	34.3	+15.4	
H_2^{gas}	6.4	41.1	−42.9	
CH_3^{gas}	46.1	62.8	−29.3	

a. Values for H and S and G are for 1200 K. Values for all surface species referenced to C_5.

Table 4

THERMOCHEMISTRY FOR TROUGH MECHANISM

SPECIES	H^a kcal/mole	S^a cal/mole-Kelvin	G^a kcal/mole	n_s
C_6HH	+11.4	+21.0	−13.8	1
C_6H^*	+51.7	+19.5	+28.4	1
C_6^*H	+46.1	+19.9	+22.2	1
C_6^{**}	+90.0	+18.4	+68.0	1
C_6HM	+26.9	+40.3	−21.5	3
C_6HM^*	+65.8	+40.1	+17.7	1
C_6^*M	+53.3	+38.9	+6.5	3
C_6B	+40.9	+26.9	+8.7	1

a. Values for H and S and G are for 1200 K. Values for all surface species referenced to C_5.

Captions

1. Comparison of measured growth rates with growth rates predicted from numerical simulations [20–22] using the trough mechanism [2]. The environments simulated were an oxygen-acetylene flame [24] (solid squares), a 220 torr DC arcjet [23] (open circle), an atmospheric-pressure RF torch [21] (open squares), a 40 Torr acetylene-oxygen flat flame [25] (solid triangle), and a hot-filament system [22] (solid circle). The calculations use the parameters given in the paper proposing the BCN mechanism [2] with the exception of the rate constant for H atom recombination at radical sites. This value was adjusted from 10^{14} to 5×10^{13} cm^3/mole-s because the former value implies a recombination rate equal to twice the collision rate.

2. The diamond slab used as the model compound for calculating steric repulsion energies.

3. Surface structures considered in this work. The letters A, B, C, and D represent adducts on the crystal slab.
   (a) C_5 ($A = H$); C_5^* ($A =^*$); C_5M ($A = CH_3$); C_5M^* ($A = CH_2^*$).
   (b) C_d^*.
   (c) C_6^* ($B =^*$); C_6 ($B = H$).
   (d) C_6 eclipsing a C_6T^*.
   (e) C_6HH ($C = H$, $D = H$); C_6H^* ($C = H$, $D =^*$);
   C_6HM ($C = H$, $D = CH_3$); C_6^*M ($C =^*$, $D = CH_3$);
   C_6HM^* ($C = H$, $D = CH_2^*$); C_6^{**} ($C =^*$, $D =^*$);
   C_6H^*H ($C =^*$, $D = H$).
   (f) C_6B.

4. Structure of a portion of the (100)-(2×1):H surface. Positions labeled *a*, *c*, *e*, and *g* are sites for addition with the dimer mechanism positions labeled *b*, *d*, *f*, and *h* are sites for addition with the trough mechanism.

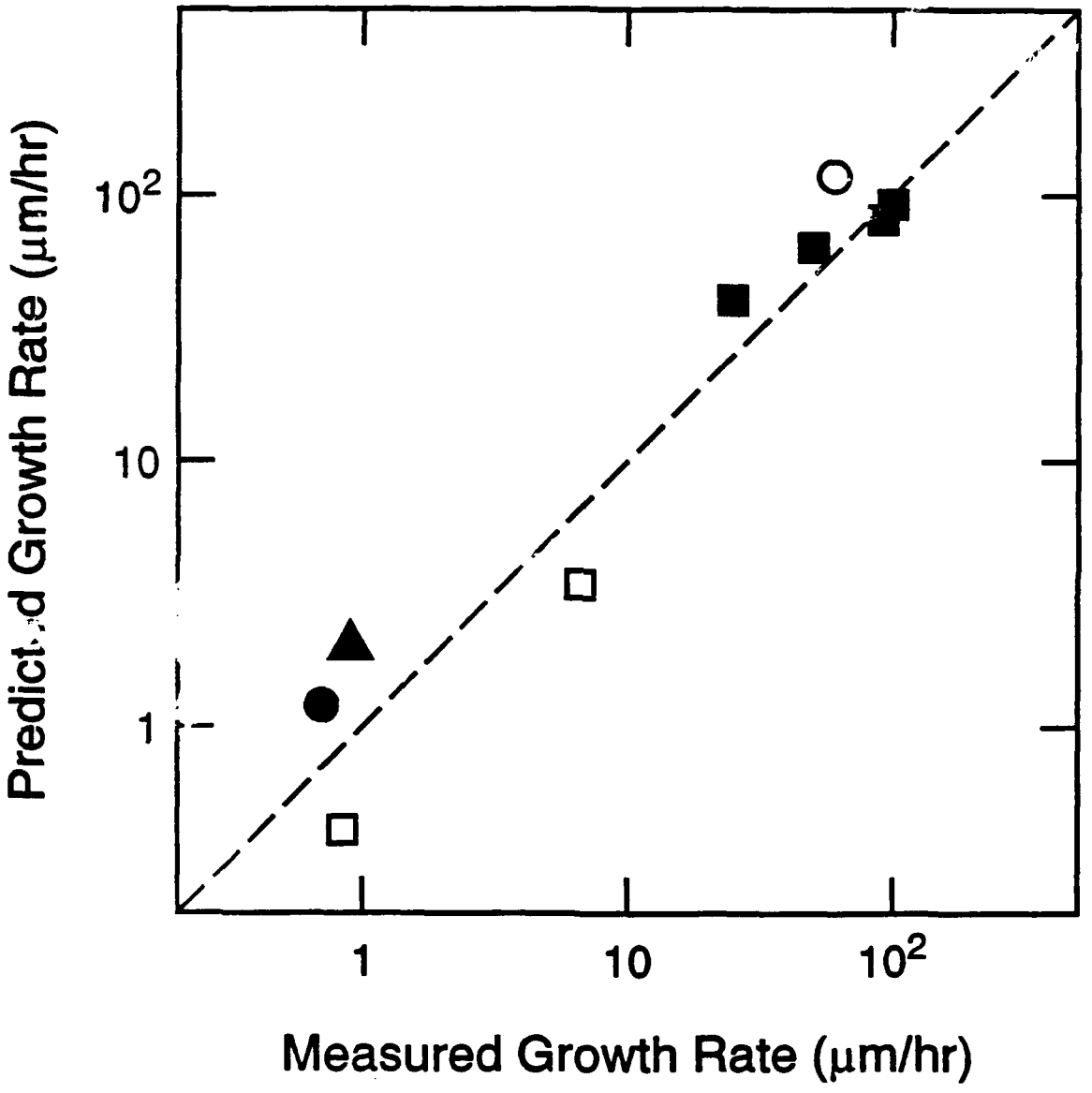
Predicted Growth Rate (μm/hr)
10²
10
1
1
10
10²
Measured Growth Rate (μm/hr)

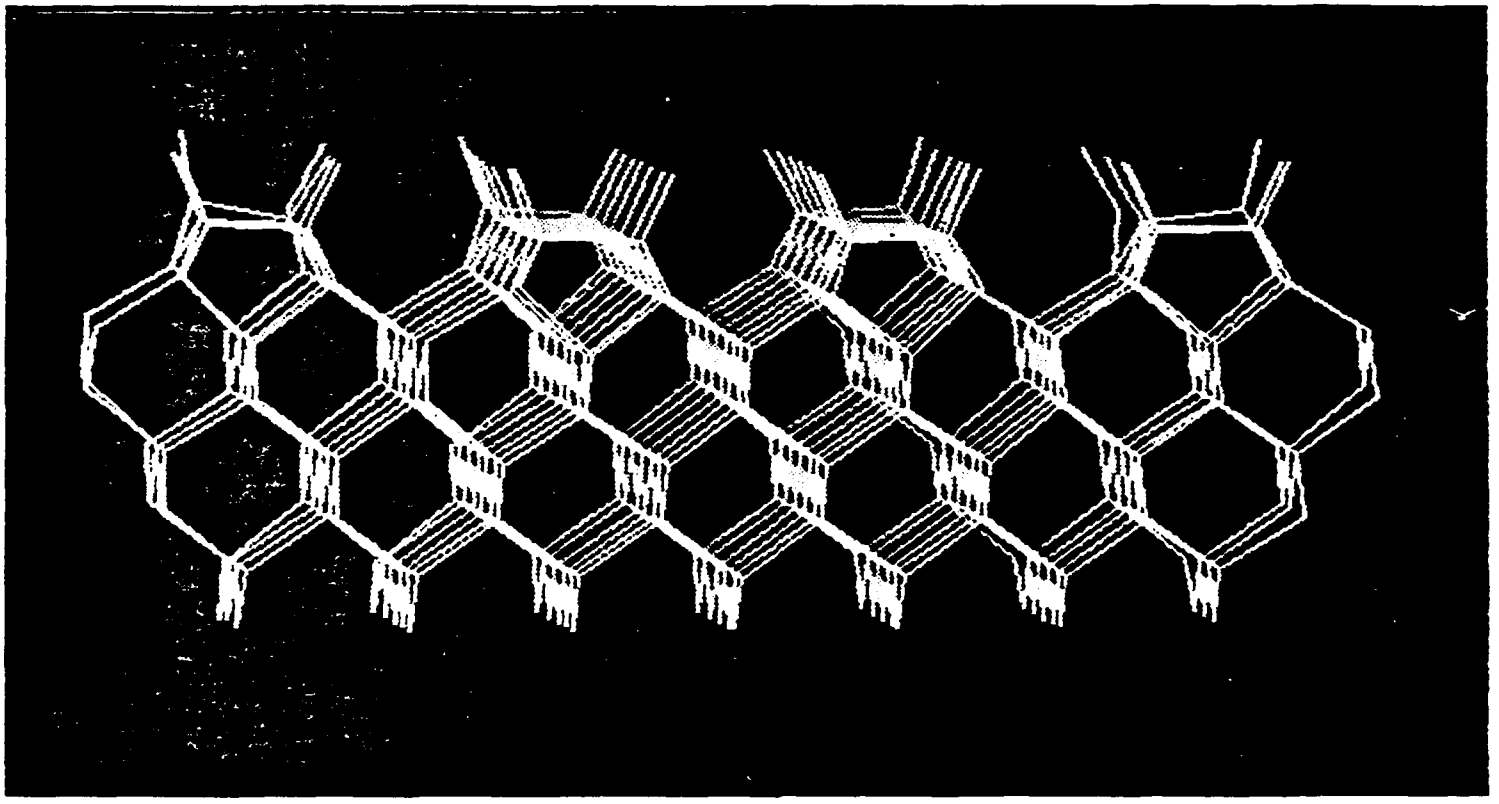

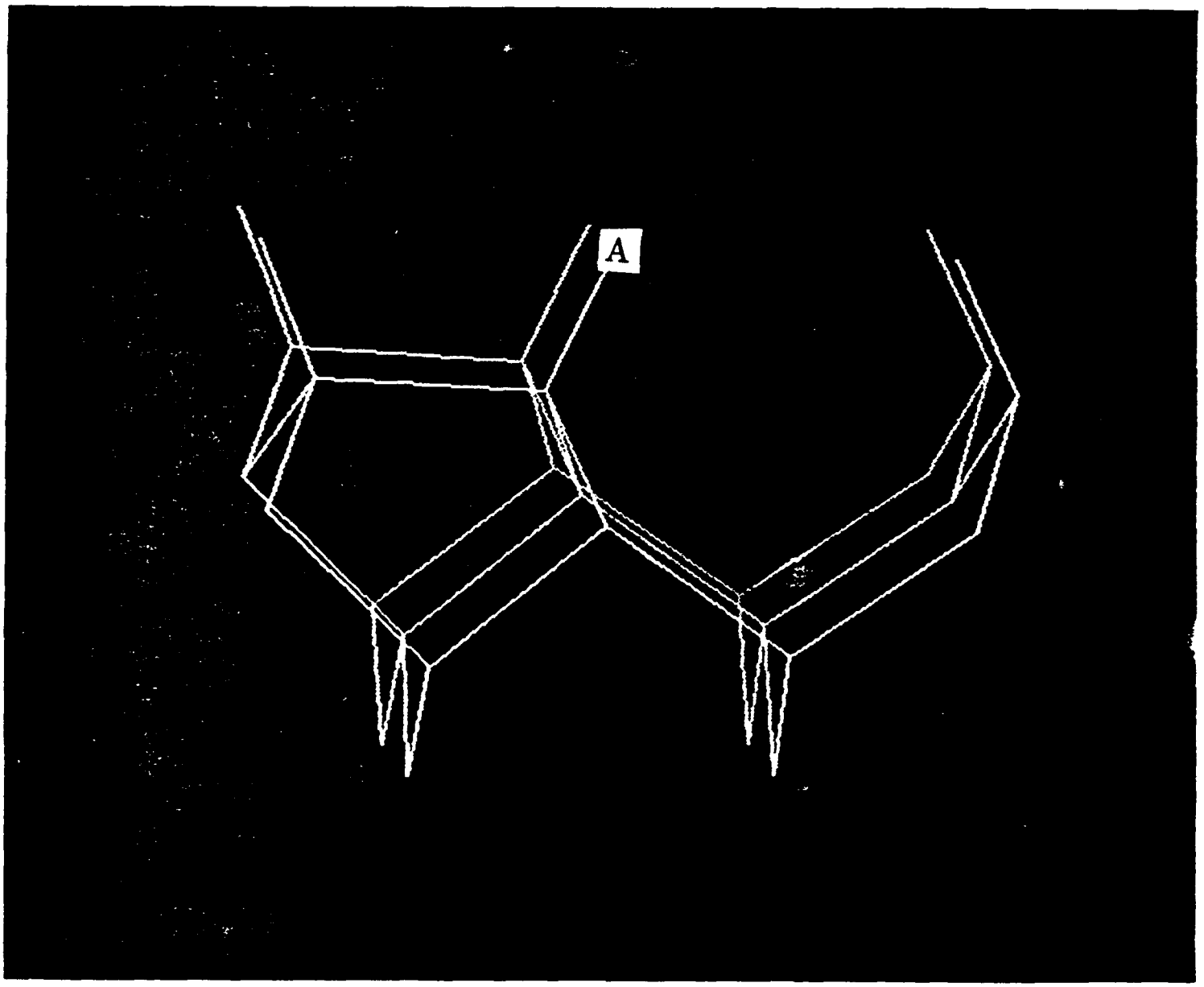
A

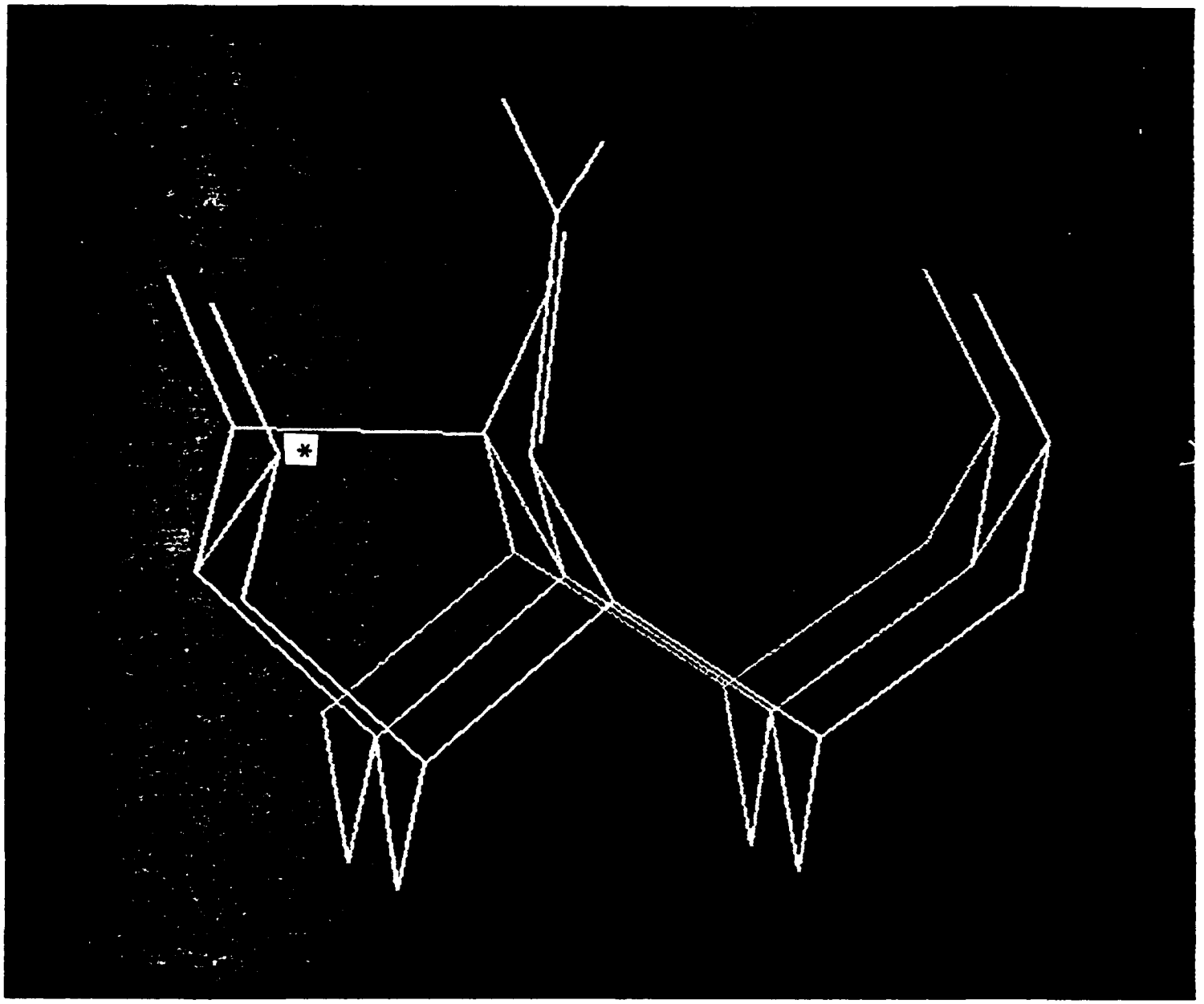

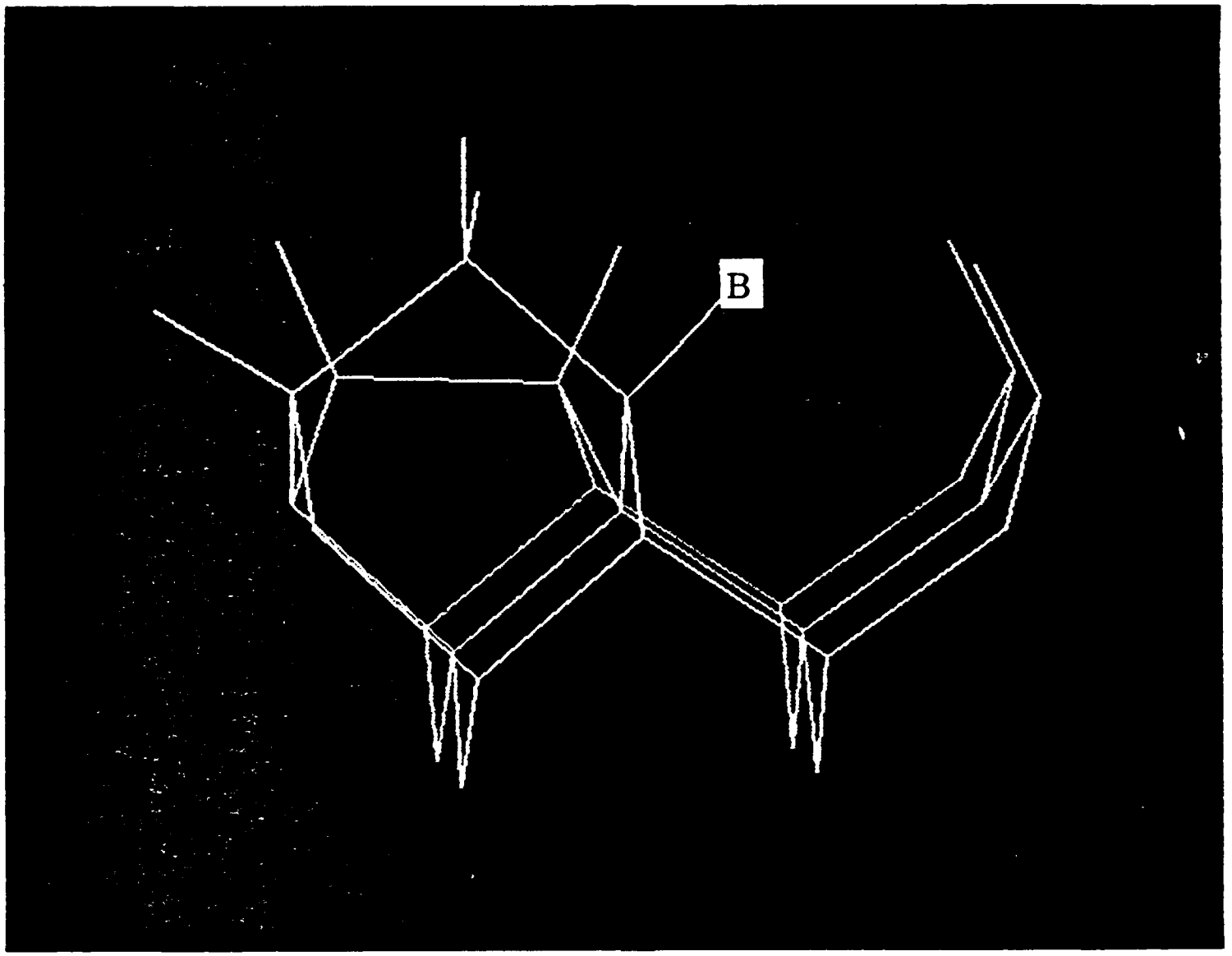
B

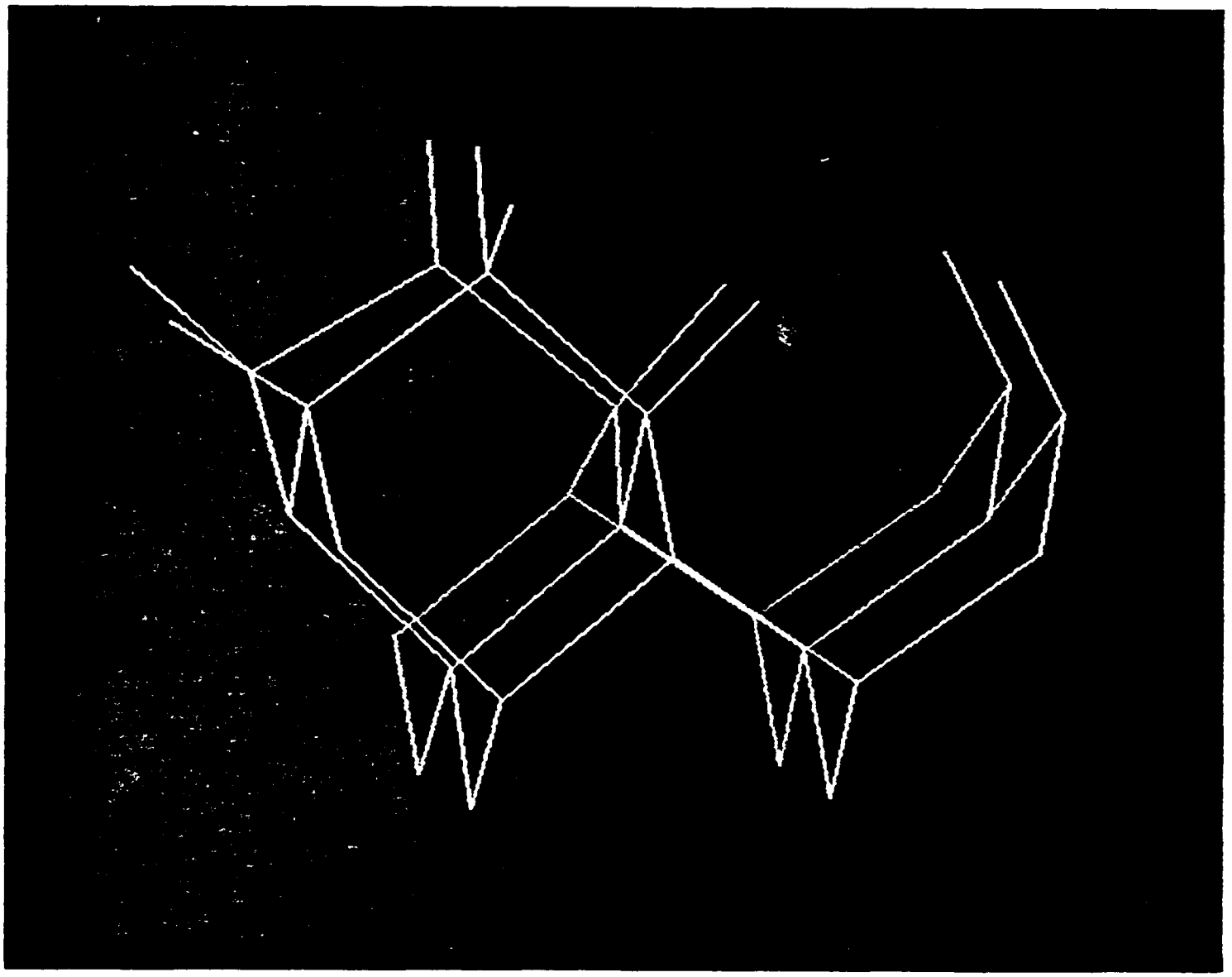

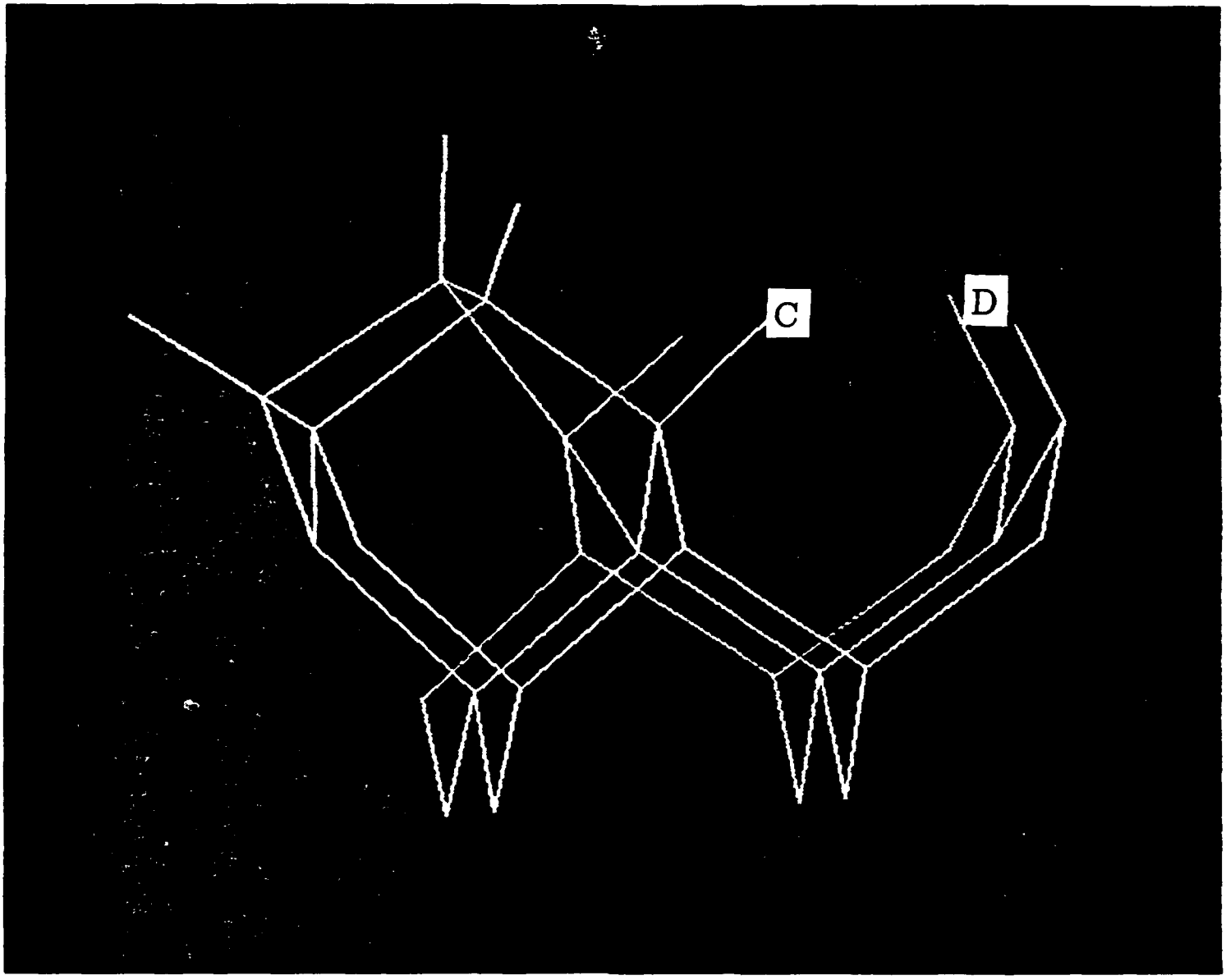
C
D

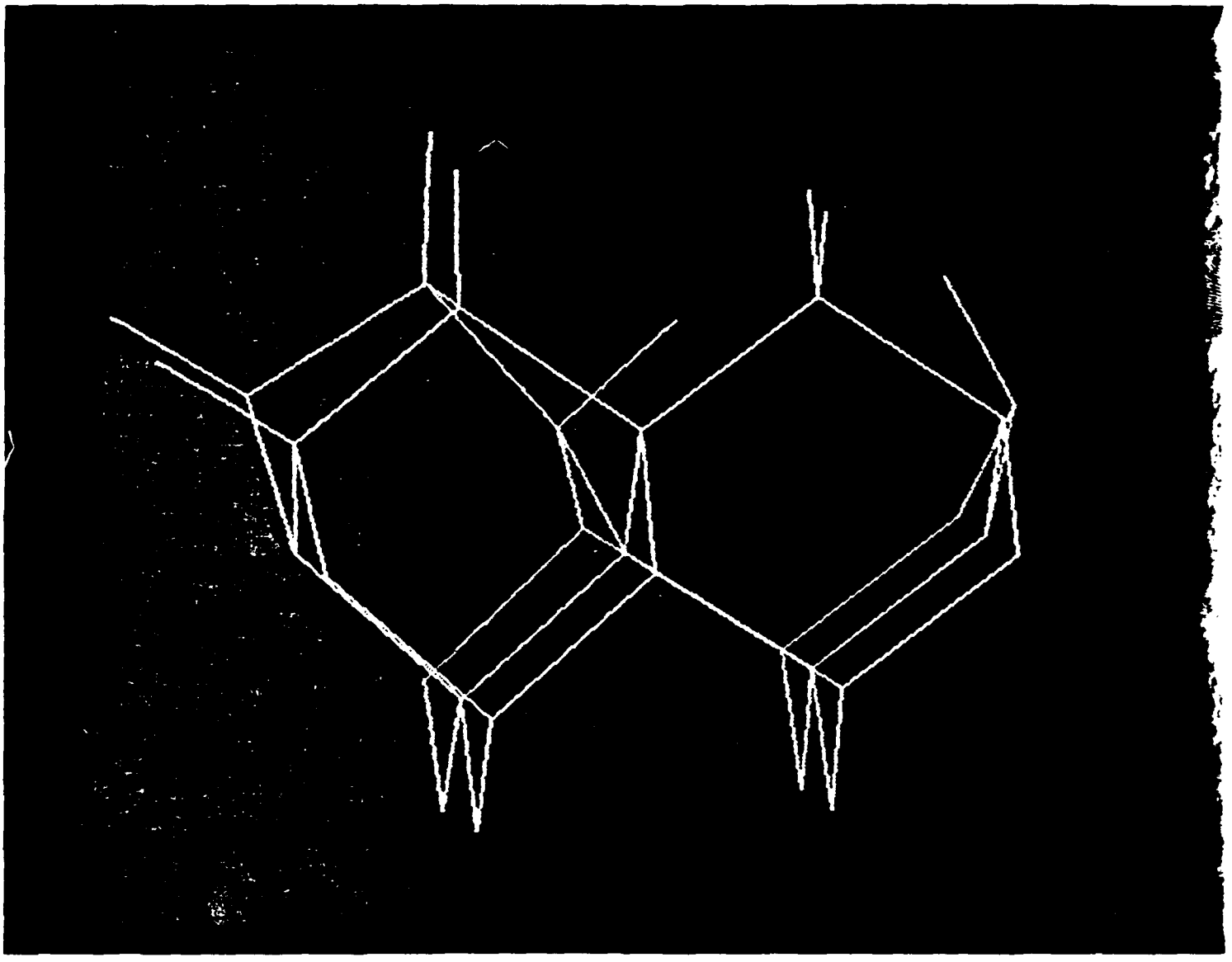

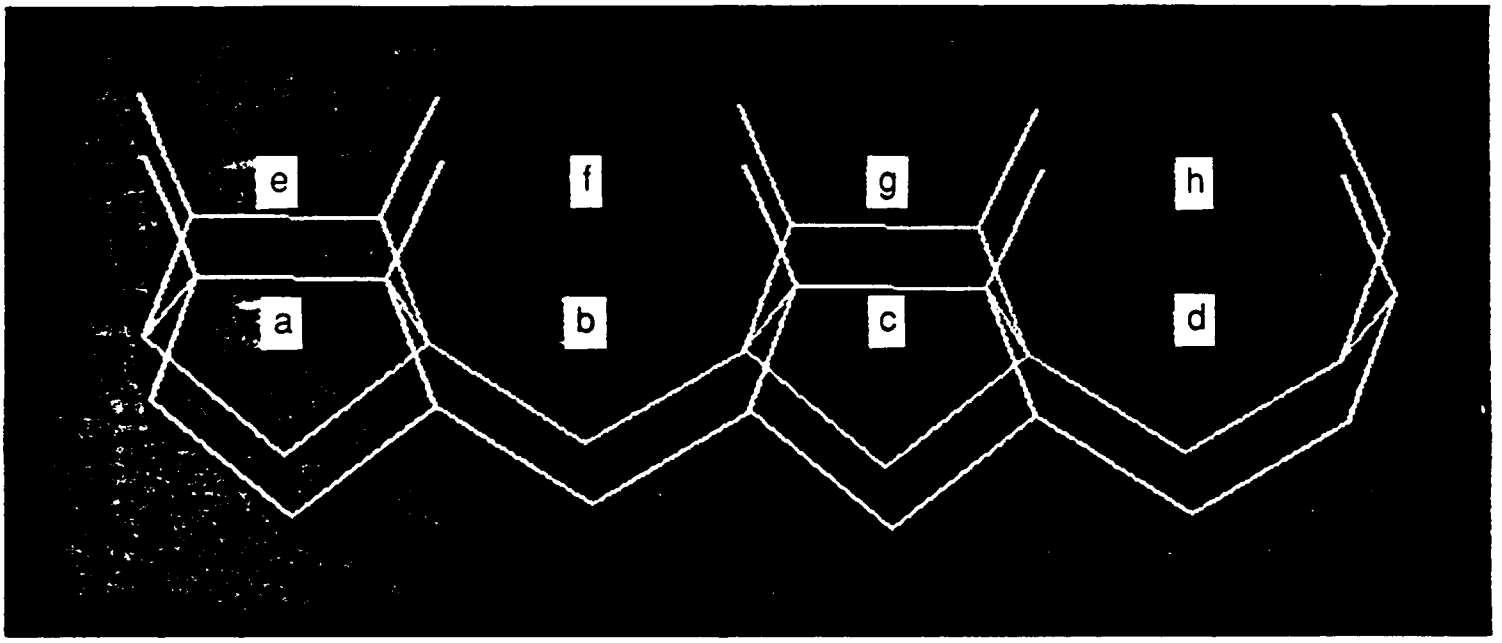
e
f
g
h
a
b
c
d

Distribution List

Mr. James Arendt
Hughes Aircraft Company
8433 Fallbrook Avenue 270/072
Canoga Park, CA 91304
(838) 702-2890

Mr. Larry Blow
General Dynamics
1525 Wilson Blvd., Suite 1200
Arlington, VA 22209
(703) 284-9107

Mr. Ellis Boudreaux
Code AGA
Air Force Armament Laboratory
Eglin AFB, FL 32542

Dr. Duncan W. Brown
Advanced Technology Materials, Inc.
7 Commerce Drive
Danbury, CT 06810-4131

Dr. Mark A. Cappelli
Stanford University
Mechanical Engineering Department
Stanford, CA 94305
(415) 723-1745

Dr. R. P. H. Chang
Materials Science & Engineering Dept.
2145 Sheridan Road
Evanston, IL 60208
(312) 491-3598

Defense Documentation Center
Cameron Station
Alexandria, VA 22314
(12 copies)

Dr. Bruce Dunn
UCLA
Chemistry Department
Los Angeles, CA 90024
(213) 825-1519

Dr. Al Feldman
Leader, Optical Materials Group
Ceramics Division
Materials Science & Engineering Lab
NIST
Gaithersburg, MD 20899
(301) 975-5740

Dr. John Field
Department of Physics
University of Cambridge
Cavendish Laboratory
Madingley Road
Cambridge CB3 OHE
England
44-223-3377333 Ext. 7318

Dr. William A. Goddard, III
Director, Materials and Molecular
Simulation Center
Beckman Institute
California Institute of Technology
Pasadena, CA 91125
(818) 356-6544 Phone
(818) 568-8824 FAX

Dr. David Goodwin
California Institute of Technology
Mechanical Engineering Dept.
Pasadena, CA 91125
(818) 356-4249

Dr. Kevin Gray
Norton Company
Goddard Road
Northboro, MA 01532
(508) 393-5968

Mr. Gordon Griffith
WRDC/MLPL
Wright-Patterson AFB, OH 45433

Dr. H. Guard
Office of Chief of Naval Research
(ONR Code 1113PO)
800 North Quincy Street
Arlington, VA 22217-5000

Dr. Alan Harker
Rockwell Int'l Science Center
1049 Camino Dos Rios
P.O. Box 1085
Thousand Oaks, CA 91360
(805) 373-4131

Mr. Stephen J. Harris
General Motors Research Laboratories
Physical Chemistry Department
30500 Mound Road
Warren, MI 48090-9055
(313) 986-1305 Phone
(313) 986-8697 FAX
E-mail: SHARRIS@GMR.COM

Mr. Rudolph A. Heinecke
Standard Telecommunication
Laboratories, Ltd.
London Road
Harlow, Essex CM17 9MA
England
44-279-29531 Ext. 2284

Dr. Kelvin Higa
Code 3854
Naval Weapons Center
China Lake, CA 93555-6001

Dr. Curt E. Johnson
Code 3854
Naval Weapons Center
China Lake, CA 93555-6001
(619) 939-1631

Dr. Larry Kabacoff (Code R32)
Officer in Charge
Naval Surface Weapons Center
White Oak Laboratory
10901 New Hampshire
Silver Spring, MD 20903-5000

Mr. M. Kinna
Office of Chief of Naval Research
(ONT Code 225)
800 North Quincy Street
Arlington, VA 22217-5000

Dr. Paul Klocek
Texas Instruments
Manager, Advanced Optical Materials Br.
13531 North Central Expressway
P.O. Box 655012, MS 72
Dallas, TX 75268
(214) 995-6865

Ms. Carol R. Lewis
Jet Propulsion Laboratory
4800 Oak Grove Drive
Mail Stop 303-308
Pasadena, CA 91109
(818) 354-3767

Dr. J.J. Mecholsky, Jr.
University of Florida
Materials Science & Engineering Dept.
256 Rhines Hall
Gainesville, FL 32611
(904) 392-1454

Dr. Russell Messier
202 Materials Research Laboratory
Pennsylvania State University
University Park, PA 16802
(814) 865-2326

Mr. Mark Moran
Code 3817
Naval Weapons Center
China Lake, CA 93555-6001

Mr. Ignacio Perez
Code 6063
Naval Air Development Center
Warminster, PA 18974
(215) 441-1681

Mr. C. Dale Perry
U.S. Army Missile Command
AMSMI-RD-ST-CM
Redstone Arsenal, AL 35898-5247

Mr. Bill Phillips
Crystallume
125 Constitution Drive
Menlo Park, CA 94025
(415) 324-9681

Dr. Rishi Raj
Cornell University
Materials Science & Engineering Dept.
Ithaca, NY 14853
(607) 255-4040

Dr. M. Ross
Office of Chief of Naval Research
(ONR Code 1113)
800 North Quincy Street
Arlington, VA 22217-5000

Dr. Rustum Roy
102A Materials Research Laboratory
Pennsylvania State University
University Park, PA 16802
(814) 863-7040 FAX

Dr. James A. Savage
Royal Signals & Radar Establishment
St. Andrews Road
Great Malvern, Worcs WR14.3PS
England
01-44-684-895043

Mr. David Siegel
Office of Chief of Naval Research
(ONT Code 213)
800 North Quincy Street
Arlington, VA 22217-5000

Dr. Keith Snail
Code 6520
Naval Research Laboratory
Washington, DC 20375
(202) 767-0390

Dr. Y. T. Tzeng
Auburn University
Electrical Engineering Department
Auburn, AL 36849
(205) 884-1869

Dr. Terrell A. Vanderah
Code 3854
Naval Weapons Center
China Lake, CA 93555-6001
(619) 939-1654

Dr. George Walrafen
Howard University
Chemistry Department
525 College Street NW
Washington, DC 20059
(202) 806-6897/6564

Mr. Roger W. Whatmore
Plessey Research Caswell Ltd.
Towcester Northampton NN128EQ
England
(0327) 54760

Dr. Charles Willingham
Raytheon Company
Research Division
131 Spring Street
Lexington, MA 02173
(617) 860-3061

Dr. Robert E. Witkowski
Westinghouse Electric Corporation
1310 Beulah Road
Pittsburgh, PA 15235
(412) 256-1173

Dr. Aaron Wold
Brown University
Chemistry Department
Providence, RI 02912
(401) 863-2857

Dr. Walter A. Yarbrough
260 Materials Research Laboratory
Pennsylvania State University
University Park, PA 16802
(814) 865-2326

Mr. M. Yoder
Office of Chief of Naval Research
(ONR Code 1114SS)
800 North Quincy Street
Arlington, VA 22217-5000

Dr. Dan Harris
Code 3854
Naval Weapons Center
China Lake, CA 93555